J. Indian Chem. Soc.,
Vol. 90, April 2013, pp. 505-511

Adsorptive removal of adipic acid from their aqueous waste over alkali activated power plant fly ash

M. Dakshene[a], A. Rani[b]* and P. D. Sharma[c]

[a]Department of Chemistry, Govt. College, Kota-324 002, Rajasthan, India

[b]Department of Pure & Applied Chemistry, University of Kota, Kota-324 002, Rajasthan, India

[c]Department of Chemistry, University of Rajasthan, Jaipur-302 004, Rajasthan, India

E-mail : monika.dakshene@gmail.com, ashu.uok@rediffmail.com, pdsjaipur@indiatimes.com
Fax : 91-744-2472960

Manuscript received 06 September 2011, revised 22 May 2012, accepted 07 June 2012

Abstract : Adipic acid is a chemical that is commonly used in the production of lubricant component, plasticizers, pharmaceutical, and rubber industries. Effluents emitted from these industries contain this chemical. It is a major cause of pollution in water system and is hazardous to the living beings. This chemical is reported to cause pain, tearing in eyes, skin irritation etc. Fly ash (FA) from coal burning power plant was activated chemically, used as a low cost adsorbent for the removal of adipic acid. The activated fly ash (AFA) was characterized for mineralogical, physiochemical and morphological properties by X-ray diffractograms (XRD), Fourier transform infra red spectroscopy (FT-IR) and scanning electron microscopy (SEM). Results showed that activated fly ash due to increased amorphous property possesses more activity over surface to act as a suitable adsorbent for the removal of acidic waste from individual effluents. The adsorption kinetics is well represented by first order kinetic model.

Keywords : Chemical activation, fly ash, adipic acid, adsorption.

Introduction

Adipic acid is one of the most widely used chemical in the world[1,2]. A green house gas data shows that nearly 2.3 million metric tonnes of adipic acid is produced all over the world annually[3]. It is mainly used to manufacture nylon fiber and plastic grease and as softener in rubber industries[4], wet strength resin, as a buffer in flue gas desulphurization treatment in power plants[5], plasticizers[6] and pharmaceutical industries. It is reported that adipic acid causes adverse effects on human and animal health. Its ester causes embryonic-fetal toxicity and teratogenic effect in rats[7]. Mucous membrane irritation and possibility of asthma due to adipic acid salt exposure[9], which is a major challenge for the environmentalists today.

Fly ash, a finely divided powdered byproduct from coal fired plant or biomass combustion facilities required ultimate disposal. The major constituents of fly ash are silica, alumina, iron oxide, lime, magnesia and alkali in varying amount with some unburnt activated carbon. Besides these, some minor elements such as Hg, As, Ge, Ga and traces of heavy metals (Cr, Co, Cu, Pb, Mn, Ni, Zn)[10] and rare earths may also be present in fly ash. The glassy (amorphous) siliceous spherical particulates are the active portion of fly ash. Typically, fly ash is 30–50% glass and higher glass content in the form of quartz is also present in it[10]. Other metal oxides such as Mn_2O_3, TiO_2 etc.[11] and minerals like mullite, hematite, ferrite and rutile in fly ash[12] are desirable from the point of view of reactivity.

Fly ash has been employed as a low cost adsorbent for flue gas and water cleaning[13–18] and many efforts have been made focused on heavy metals[19,20] and dye adsorption[21,22] on fly ash particles. However no investigations have been reported on organic acids. In this paper we reported the use of fly ash as an adsorbent by activating it, for the complete removal of adipic acid from aqueous waste. Batch adsorption studies were carried out systematically and attempts have also been made to understand the adsorption equilibrium and kinetics.

Results and discussion

Characterization of adsorbent :

XRD analysis :

The peaks of X-ray diffractograms of fly ash show that the fly ash sample before and after activation (Figs. 1a, b) contains quartz, mullite and calcite in large amount. X-Ray diffraction pattern of fly ash (Fig. 1a) shows the presence of crystalline phase whereas XRD pattern of activated fly ash (Fig. 1b) shows the presence of amorphous nature with little crystallinity which is due to increase in amorphous silica content after alkali treatment. The chemical activation removes most of the crystalline component present in fly ash sample and increases the amorphous nature. The crystallite size of FA decreases from 33 nm to 11 nm on alkali treatment showing

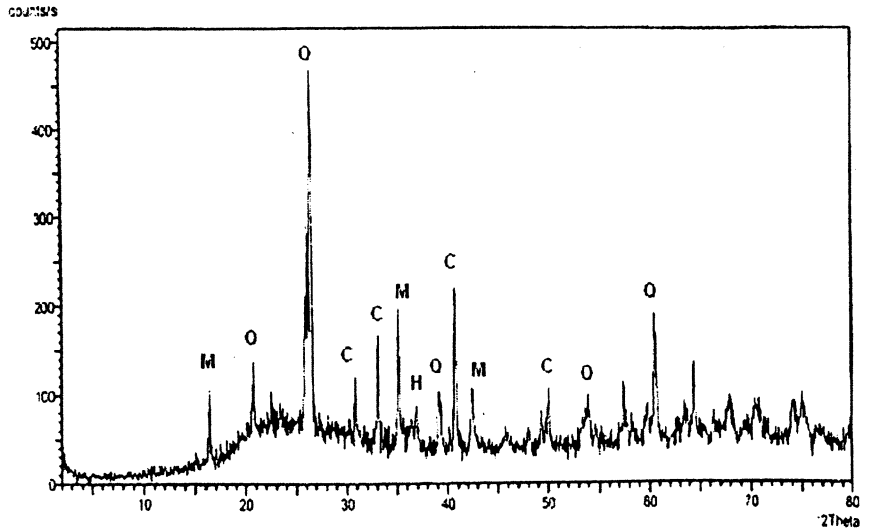

Q - Quartz, C - Calcite, M - Mullite, H - Haematite

Fig. 1(a). XRD of pure fly ash.

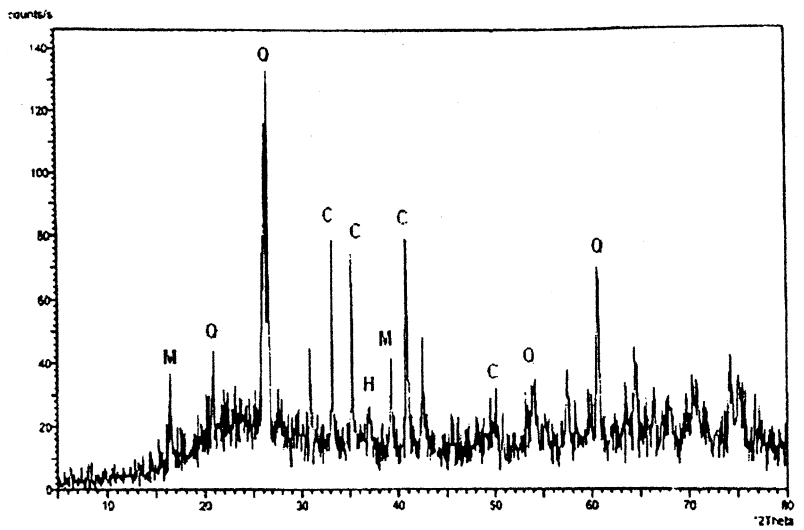

Q - Quartz, C - Calcite, M - Mullite, H - Haematite

Fig. 1(b). XRD of alkali activated fly ash.

nanocrystalline phase in the sample. Previous studies have shown that fly ash after alkali treatment gives sharp diffraction peaks that are different from those present in untreated one. The diffractograms show the original crystalline phases of fly ash, quartz and mullite are mostly absent in zeolite material after reaction[23].

SEM analysis :

Figs. 2 (a) and (b) show the scanning electron microscope picture of pure and activated FA respectively. In addition to the general physical characteristics and elemental composition of random population of fly ash, the SEM data clearly indicate intermixing of silica and alumina phases and predominance of Ca and other nonsilicate minerals. These results supported the data obtained from XRD.

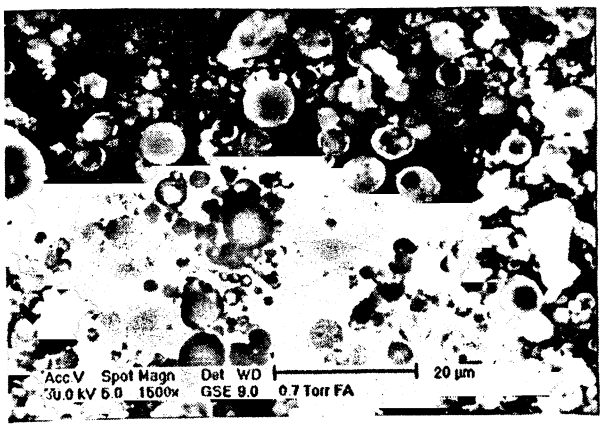

Fig. 2(a). SEM photograph of pure fly ash.

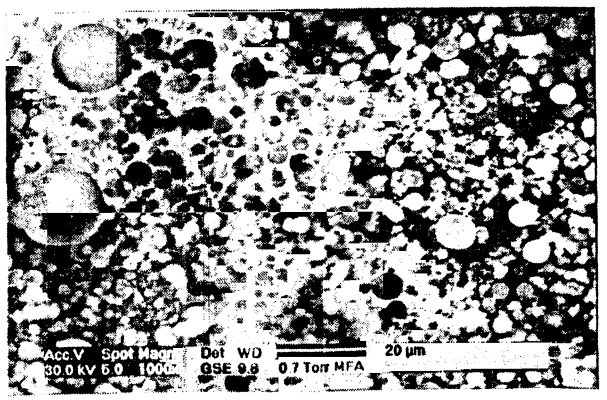

Fig. 2(b). SEM photograph of alkali activated fly ash.

Fig. 2(a) reveals that in the FA, the size of particles range from 840 nm to 10 µm and the majority of particles ranged in 1 µm to 100 µm, consisted of solid sphere, hollow cenosphere, irregularly shaped unburnt carbon particles and mineral aggregates and agglomerated particles which after alkali treatment (Fig. 2b) resulted into scattered agglomerated particles conferring the increase in amorphous property. These results supported data obtained from previous studies and were consistent with XRD data[24].

FT-IR analysis :

In alkali activation process higher concentration of -OH groups favor the breaking of Si-O-Si, Al-O-Al and Si-O-Al bonds and formation of Si-OH and Al-OH groups occur which is confirmed by a broad band between 3400–3000 cm^{-1} (Fig. 3b) attributes the presence of surfacial hydroxyl group of Si-OH and adsorbed water molecules on the surface. The broadening of a band is due to the strong hydrogen bonding. The hydroxyl groups donot exist in isolation and a high degree of association is experienced as a result of extensive hydrogen bonding with other hydroxyl groups. A peak at 1650 cm^{-1} in the spectra of both the samples is attributed to the bending mode of water molecule. Signals at 996 cm^{-1}, 1081 cm^{-1}, 1185 cm^{-1} are attributed respectively to the vitreous phase of unreacted fly ash, quartz and mullite while a new component appearing at around 1025–1006 cm^{-1} is attributed to the sodium alumino silicate[25] which is also confirmed by some previous studies[26].

TGA :

Both pure and activated fly ash samples were heated from 50 °C to 900 °C at 10 °C per minute change. There is approximately 1.9% weight loss for FA while only 0.2–3% for AFA sample. Weight loss seems to be due to moisture content and unburnt carbon loss only.

Adsorption isotherms :

To optimize the design of an adsorption system for the adsorption of adsorbate, the most appropriate correlation for the equilibrium curve is Langmuir and Freundlich. The Langmuir isotherm is valid for monolayer adsorption onto a surface containing a finite number of identical sites.

$$Q_e = \frac{Q_0 b C_e}{1 + bC_e} \qquad (A.1)$$

or

$$m/x = \frac{1}{Q_0} + \frac{1}{Q_0 b C_e} \qquad (A.2)$$

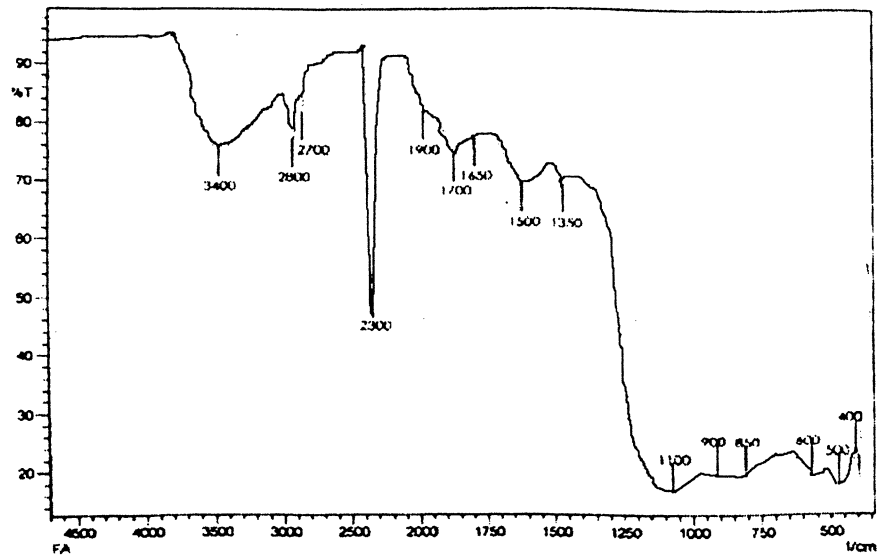

Fig. 3(a). FT-IR spectra of pure fly ash.

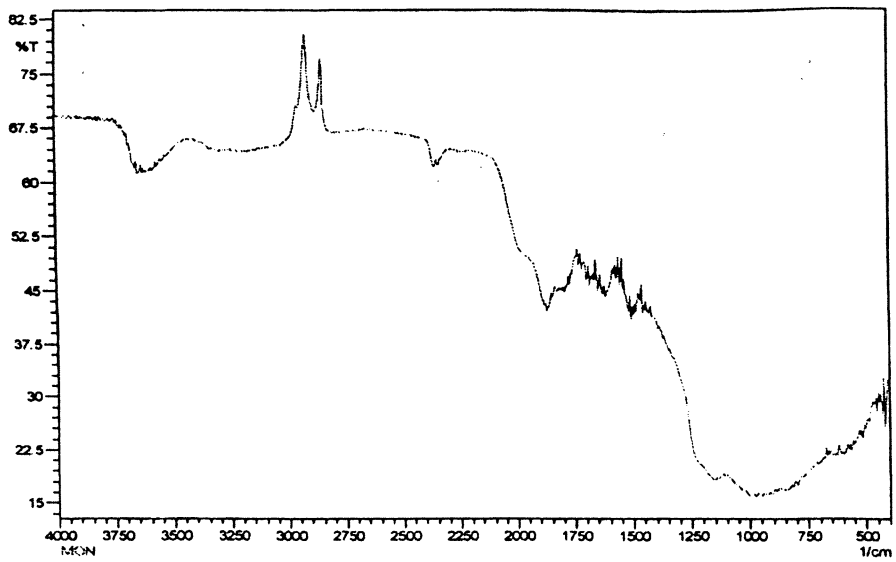

Fig. 3(b). FT-IR spectra of alkali activated fly ash.

where Q_e is the amount of acid adsorbed at equilibrium in mg/g, C_e is the equilibrium concentration in mg/L and Q_0 is the solid phase concentration corresponding to complete coverage of adsorption sites, b is the Langmuir constant, which indicates the nature of adsorption and indicates the shape of the isotherm accordingly. The essential characteristics of a Langmuir isotherm can be expressed in terms of a dimensionless separation factor (r)[27,28], which describes the type of isotherm and is defined by eq. (3).

$$r = \frac{1}{1 + bC_0} \qquad \text{(A.3)}$$

Linearised Freundlich adsorption isotherm equation is given by eq. (3).

$$\log q_e = \log K_f + 1/n \log C_e \qquad \text{(A.4)}$$

where q_e is the amount of acid adsorbed per unit weight of adsorbent (mg/g), K_f and $1/n$ are the Freundlich constants related to adsorption capacity and intensity respectively.

The Langmuir plots are linear, shown in Fig. 4(a). The plots of Freundlich isotherm yield a straight line of slope $1/n$ and intercept log K_f. It is clear from Table 1 that the r values for the present experimental plot favors the adsorption of adipic acid on alkali activated fly ash.

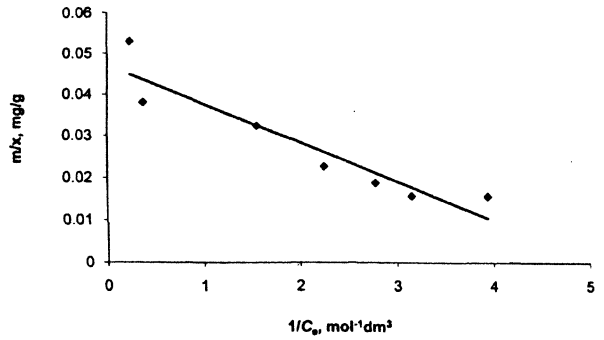

Fig. 4(a). Langmuir plot.

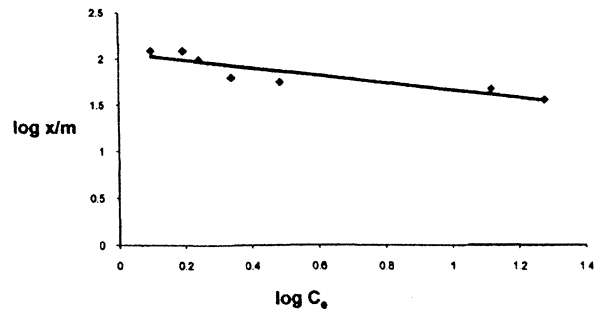

Fig 4(b). Freundlich plots.

Table 1. Values of Langmuir and Freundlich constants for adipic acid adsorption over AFA at different [acid] at 30 °C

10^3 [acid]	Langmuir constants				Freundlich constant	
(mol dm^{-3})	b	r	Q_0	R^2	K_f	$1/n$
5	1.045	0.18	39.37	1.0	117.5	0.3984
10	0.528	0.18	76.92	1.0	151.5	0.3992
50	0.100	0.19	169.4	1.0	1893.6	0.4921

Kinetics of adsorption :

Kinetics of adipic acid removal over AFA is studied by varying concentration of adipic acid, AFA and temperature.

Time vs percentage adsorption graph shows (Fig. 5) initial rapid adsorption. Initial slope is used for determining initial rate (R_{obs}). From the log-log plot of R_{obs} vs adipic acid and R_{obs} vs AFA, an order of 1.0 and 0.5 ± 0.03 is achieved respectively. The functional dependence of rate on [acid] and [AFA], the final rate law is,

$$R_{obs} = K\,[(CH_2)_4(COOH)_2]\,[AFA]^{0.5} \qquad (B.1)$$

The value of K is calculated 0.46 ± 0.23 g$^{-0.5}$ dm$^{1.5}$ s^{-1} from the plot of R_{obs} with $[AFA]^{0.5}$.

Temperature was varied from 25 °C to 35 °C. The values of k determined at different temperature were used in Arrhenius equation. From the plot of log k against $1/T$, the value of activation energy was calculated to be 39.15 ± 1.95 kJ mol^{-1}.

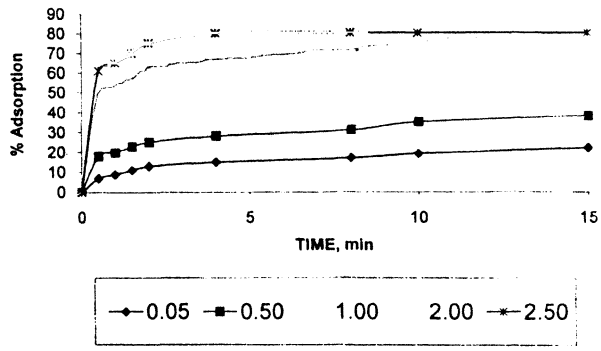

Fig. 5. Change in % adsorption of adipic acid with time at different [AFA] at 30 °C.

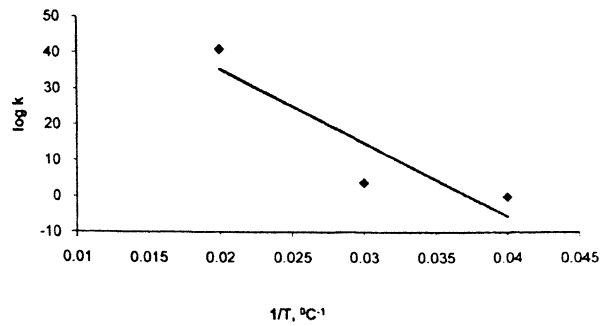

Fig. 6. Arrhenius equation plot for adipic acid adsorption.

The above adsorption kinetics was modeled on five different models. All models were tested with least square regression analysis. The adsorption data were also fitted at five different kinetic models viz. zero order, first order, Elovich equation, parabolic diffusion equation and two rate constants. The values of slope, correlation coefficient (R^2) and standard errors of estimate (SEE) are given in Table 2. On the basis of high R^2 and low SEE, the most favorable model to describe the adsorption kinetics is first order kinetic model (Fig. 7). While parabolic diffusion and two rate constant models are com-

Table 2. Coefficient of determination (R^2), standard error of estimate (SEE), and slope for graphical equation of different kinetic models applied on adipic acid adsorption on [AFA] at 30 °C

[Acid] = 5 × 10^{-3} mol dm^{-3}, [AFA] = 2 g dm^{-3}

Kinetic models	R^2	SEE	Slope
Zero order	0.744	0.23569	-0.07
First order	0.9453	0.21034	-0.2182
Elovich equation	0.6073	0.12509	-0.0886
Parabolic diffusion	0.5922	0.41016	-0.4199
Two rate constant	0.7419	0.03100	-0.021

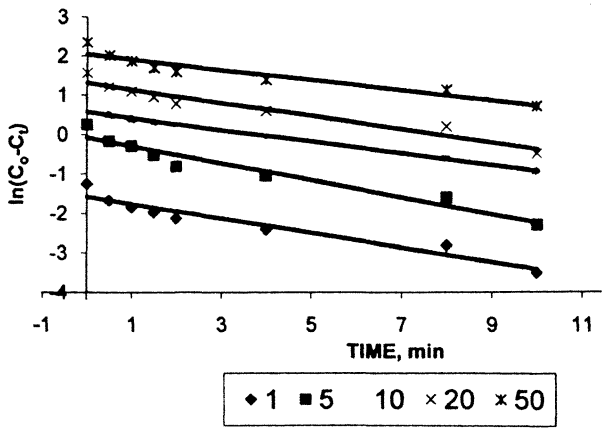

Fig. 7. First order equation plots for adipic acid adsorption at different [Acid]. [AFA]= 2.0 g dm^{-3}, Temp. = 30 °C.

pletely rejected. Values of statistical parameters for different examples are given in Table 2.

Experimental

Materials and methods :

Class F fly ash (a pozzolanic material that contains 70% SiO_2, Al_2O_3 and Fe_2O_3 with 5% SO_3 and 3% of moisture content as defined in ASTM C618), collected from KSTPS (Kota Super Thermal Power Plant), Rajasthan, was dried and sieved to obtain uniform particle size sample. Stock solution of adipic acid of BDH make was prepared by doubly distilled water. Phenolphthalein was used as an indicator in this study.

Catalyst synthesis :

The catalyst has been synthesized by adding 60 mL of 0.05 *N* NaOH to 40 g of pure fly ash sample. Chemical activation was carried out by continuous stirring of a mixture (NaOH and FA) for 3 h at 90 °C then washed to a neutral pH and dried in an oven.

Characterization :

Both the initial i.e. pure fly ash (FA) and the residue obtained after alkaline treatment i.e. activated fly ash (AFA) were characterized mineralogically and microstructurally. Philips Expert XRD used for determining crystallite size. Samples were scanned at 2θ range of 0–80° at a scanning rate of 0.04 s^{-1} [29]. FT-IR spectra of both the samples were recorded in the range 400–4000 cm^{-1} with a resolution of 4 cm^{-1}. Specific surface area, pore volume and pore size in the sample were determined from N_2 adsorption-desorption isotherms using model NOVA 1000E surface area at 77 K. Thermogravimetric analysis (TGA) was done in the temperature range 50 °C to 1000 °C using model Mettler Toledo. To determine the morphology, external surface structures and external elemental distribution of individual FA particle, scanning electron microscope (Philips XL 30 ESEM TMP) has been used.

Adsorption kinetics :

In the batch method, 50 mL of adsorbate solution was taken into an Erlenmayer flask and allowed to attain the desired temperature by circulating thermostated water around the reaction vessel. To initiate the reaction, a fixed amount of adsorbent (2 g/dm^3) was added and stirred continuously at about 1400 ± 1 rpm. The kinetics was followed by withdrawing 0.05 dm^3 aliquot sample at different intervals. The adsorbent was separated from aliquot by simple filtration. Concentration of adipic acid was then estimated, titrating with standard NaOH solution using phenolphthalein as an indicator. Temperature was varied for estimating activation energy. Experimental runs were observed with initial rapid adsorption trends for a period of 0.5 min to 2.5 min.

Conclusion :

The adsorption catalyst AFA synthesized during this work is found to have sufficient activity to remove adipic acid. Kinetic rate law has given first order with respect to initial concentration and a fractional order of 0.5 ± 0.03 for [AFA] at 30 °C. A high value of activation energy indicates that chemisorption is to be important in case of using AFA than physisorption. The study generates fly ash catalyst for waste water treatment in lubricants, plasticizer, pharmaceutical industries etc. where adipic acid remains as waste in the effluent.

Acknowledgement

The authors are thankful to Dr. D. D. Phase and Er. V. K. Ahiray for SEM analysis, conducted at UGC DAU-CSR Lab, Indore. The financial support was provided by Fly Ash Unit, Department of Science and Technology, New Delhi, India, vide project sanction no. FAU/DST/600(23)/2009-10.

References

1. A. Castellan, J. C. J. Bart and S. Cavallaro, *J. Catalysis Today*, 1991, **9**, 237.
2. D. D. Davis, "Adipic Acid", in : 'Kirk-Othmer, Encyclopedia of Chemical Technology', 4th ed., John Wiley and Sons, 1991, Vol. 1, 466.
3. Haskell Laboratory Duport Company, *Toxicity of Adipic Acid*, 2002, **25**, 191.
4. Whelan Tony, Polymer Technology Dictionary, 1994, Technology.
5. D. D. Davis, "Adipic Acid", in : 'Ullmann's Encyclopedia of Industrial Chemistry', 5th revised ed., VCH Verlagsgesellschaft, 1985, Vol. A1, 269.
6. E. Eckard Robert, *Env. Health Perspective*, 1976, **17**, 103.
7. A. R. Singh, H. Lawrence and J. Autiun, *J. Pharm. Sci.*, 2006, **62**, 1596.
8. M. A. Krapotkina, Gigiena Truda, Professional Nye Zabolevaniya, 1981, **5**, 46 (English translation).
9. Z. Lu, PhD Thesis, Pensylvania State University, 2002.
10. S. Gomes and M. François, *Cem. Conor. Res.*, 2000, 175.
11. I. Garcia-Lodeiro, A. Palomo and A. Fernandez-Jimenez, *Cem. Conor. Res.*, 2007, **37**, 175.
12. H. Pengwei, Y. Yongsheng, L. Songtian, L. Huaming, and W. Huang, *Desalination*, 2010, **256**, 196.
13. J. R. Kastener, N. D. Melear and K. C. Das, *J. Hazard. Mater.*, 2002, **95**, 81.
14. G. Q. Lu and D. D. Do, *Fuel Process Technol.*, 1991, **27**, 95.
15. T. R. Carry, C. F. Richardson, R. Chang, F. B. Meserole, M. Rostam Abadi and S. Chen, *Environ. Prog.*, 2000, **19**, 167.
16. O. Malerius and J. Werther, *Chem. Eng. J.*, 2003, **96**, 197.
17. A. Peloso, M. Rovatti and G. Ferraiolo, *Resour. Conserv.*, 1983, **10**, 211.
18. K. K. Panday, G. Prasad and V. N. Singh, *Water Res.*, 1985, **19**, 869.
19. A. K. Sen and A. K. De, *Water Res.*, 1987, **21**, 885.
20. D. Mohan, K. P. Singh, G. Singh and K. Kumar, *Ind. Eng. Chem. Res.*, 2002, **41**, 3688.
21. P. Janos, H. Buchtova and M. Ryznarova, *Water Res.*, 2003, **37**, 4938.
22. B. D. Cullity and S. R. Stock, "Elements of X-Ray Diffraction", 3rd ed., 2001.
23. Keka Ojha, C. Narayan Pradhan and Amarnath Samanta, *Bull. Mater. Sci.*, 2004, **27**, 555.
24. B. G. Kutchko and A. G. Kim, *Fuel*, 2006, **85**, 2537.
25. A. Fernandez-Jimenez and A. Palomo, *Microporous and Mesoporous Mater.*, 2005, **86**, 207.
26. A. Fernandez-Jimenez, M. Monzo, M. Vincent, A. Barba and A. Palomo, *Microporous and Mesoporous Mater.*, 2008, **108**, 41.
27. T. W. Weber and Chakravorti, *J. Am. Ins. Chem. Eng.*, 1974, **2**, 228.
28. N. Kanan and M. Meenakshi Sundaram, *Ind. J. Env. Protec.*, 2002, **22**, 9.
29. M. T. Postek, K. S. Howard, A. H. Johnson and K. L. Mc. Michael, "Scanning Electron Microscopy : A Students Handbook Burlington", Ladd Research Industries, 1980.